Electronic Supplementary Material (ESI) for Journal of Materials Chemistry A.

Supporting information

Unveiling the Mechanism on Photocatalytic Singlet Oxygen Generation Over Rationally Designed Carbonylated Carbon Nitride

Wei Liu[a], Huinan Che[a], Bin Liu[b] and Yanhui Ao[a*]

W. Liu, H.N. Che, Prof. Y. H. Ao

[a]Key Laboratory of Integrated Regulation and Resource Development on Shallow Lakes, Ministry of Education, College of Environment, Hohai University, No.1, Xikang road, Nanjing, 210098, China

Prof. B. Liu

[b]Department of Materials Science and Engineering, City University of Hong Kong, Hong Kong SAR 999077, China

**Corresponding author* E-mail: andyao@hhu.edu.cn

1.1 Chemicals reagents and materials

Melamine (99%), 3,3’,5,5’-tetramethylbenzidine (TMB), superoxide dismutase (SOD), mannite, catalase, and tryptophan, absolute ethanol, barium sulfate ($BaSO_4$), and potassium bromide (KBr) were obtained from Aladdin Chemical Reagent (Shanghai) Co., Ltd. Concentrated sulfuric acid and concentrated nitric acid were obtained from Sinopharm Chemical Reagent Co., Ltd. All chemicals reagents and materials were used as received without further purification

1.2 Synthesis of samples

the pristine PCN samples were prepared by polymerization of melamine molecules under high temperature. In detail, 10 g of melamine was put into a crucible with a cover and heated at 550 °C for 4 h in a tube furnace with a ramp rate of 5 °C/min. After being cooled down, the obtained yellow product was collected and fully ground, yielding the power samples denoted PCN. Finally, we weighed the sample and obtained 5.4226 g of PCN.

1.3 Synthesis of carbonylated carbon nitride (Ox-CN)

The Ox-CN samples were prepared by oxidation treatment of pristine polymer carbon nitride. In detail, 1g of PCN powder was carefully added into the mixture of 50 mL concentrated sulfuric acid and 100 mL concentrated nitric acid. After being agitated overnight, the mixture was poured into 500 mL distilled water and collected by extraction filtration. The yellow-white product was washed with distilled water for several times and dried in air at room temperature, yielding the power samples denoted Ox-CN. Finally, we weighed the sample and obtained 0.8962 g of Ox-CN.

1.4 Photocatalysis experiment

1.4.1 Molecular Oxygen activation experiment

12.5 mg of samples were added into 50 mL of HAc/NaAc buffer solution aqueous, then 1mL of TMB (25 mM) aqueous solution was poured into the mixture solution. A xenon lamp (CEL-HXF 300, Beijing China Education Au-light Co., Ltd) without filter was used as the light source. The oxidation of TMB molecules was evaluated by monitoring the absorbance of the mixture solution with a UV-vis spectrophotometer. The measurements were performed under various atmospheres to assess molecular oxygen activation properties. TMB measurements with different scavengers (tryptophan, 125 mg; mannite, 22.75 mg; catalase, 50mg; SOD, 0.4 g/L, 500 μL) were performed to identify active oxygen species.

1.4.2 Photocatalysis degradation experiment

The photocatalytic active of the synthesized photocatalysts was evaluated by degradation of SMX under a 300 W xenon lamp without filter (CEL-HXF 300, Beijing China Education Au-light Co., Ltd). Typically, 20 mg of samples were added into 100 mL beaker containing 50 mL of 5 mg/L SMX aqueous. After ultrasonic treatment of 10 min, the suspension was magnetically stirred in dark for 20 min to reach adsorption-adsorption equilibrium between pollutant and photocatalyst. Meanwhile, the Xenon lamp needs to idle away for 20 min to maintain stable light output. And the temperature of the reactor was maintained at 25 °C. Then, at a set time interval, 2 mL of solution was taken and filtered via a 0.22 μm nylon membrane to remove sediment. All the experiments were carried out at least duplicate. The SMX concentration was determined by high-performance liquid chromatography equipped with a C18 column and a UV-vis detector (Waters e2695). The column temperature was held at 25 °C. The volume of injection was 10 μL. The mobile phase was acetonitrile/water (2:3) at a flow rate of 1.0 mL/min, and the detection wavelength was set at 254 nm with peak time at about 5 min.

1.5 Characterization

The crystal phase of as-obtained samples was determined by X-ray diffraction (XRD, Rigaku, Smart-Lab). The chemical composition was studied by X-ray photoelectron spectroscopy (XPS, ESCALAB250XI, America) Transmission electron microscopy (TEM, JEOL, JEM-F200) were used to survey the morphology and structure. The High-angle annular dark-field scanning transmission electron microscopy (HAADF-STEM) was tested by transmission electron microscopy (TEM, Tecnai G2 F30 S-TWIN). The specific surface area of as-prepared samples was investigated by N_2 adsorption-desorption (Micromeritics ASAP 2460, America). Transient Photoluminescence (PL) profiles were performed on Fluorescence Spectrophotometer F-7000 (Hitachi, Japan) with a 360 nm laser excitation source. The diffuse reflectance absorption spectra (DRS) of as-obtained samples were analyzed on a UV-vis spectrophotometer (UV-3600, Shimadzu Corporation, Tokyo, Japan) and $BaSO_4$ was regarded as reference.

1.6 DFT Calculations

The geometry optimization and excited-state calculations were performed by ub3lyp exchange-correlation functional with the 6-31G(d) basis set based on Gaussian 16 C.01 code [1]. Frequency calculations were performed to ensure that the stability configuration has no imaginary frequency. The solvent effect of H_2O was considered using self-consistent reaction field (SCRF) based on the solvation model density (SMD) implicit solvent model [2]. Frontier molecular orbital, density of states (DOS) were calculated with Multiwfn 3.8 (dev) [3]. All structures and iso-surfaces images were visualized by VMD 1.9.3 [4]. The single-point energy was calculated by using PWPB95-D3(BJ) double-hybrid functionals in conjunction with the def2-TZVPP basis set based on ORCA 5.2.1 [5]. The adsorption energy (Eads) of O_2 was calculated as follows:

$$E_{ads}(*O_2) = E(*O_2) - E(*) - E(O_2)$$

Where E(*O_2), E(O_2), and E (*) are the total energy of samples with O_2 adsorbates on the surface, the energy of pristine samples surface and O_2, respectively.

At room temperature, the Gibbs free energy for each model was calculated by the following equation:

$$G(T) = E_{ele} + G_{corr}(T) = E_{ele} + ZPE + \Delta G_{0\rightarrow T}$$

Where E_{ele}, $G_{corr}(T)$, ZPE and $\Delta G_{0\rightarrow T}$ were electronic energy, thermal corrections to Gibbs free energy, zero-point-energy and contribution by heating the system from 0 K to 298.15 K.

Supporting information

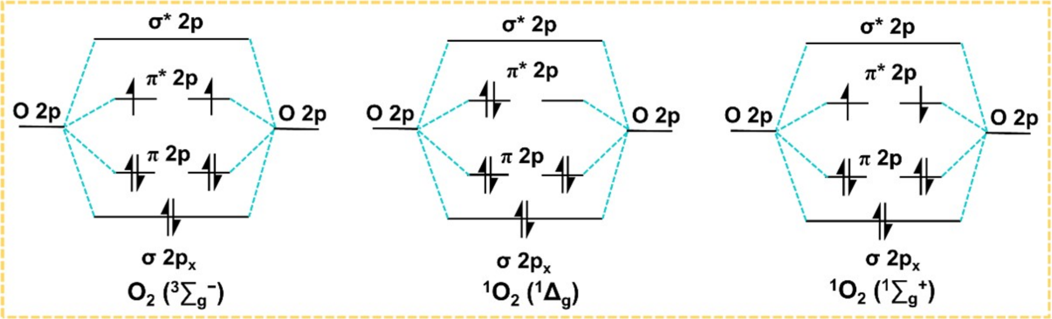

Figure S1. Molecular orbital structure of $^3O_2(^3\sum_g^-)$, $^1O_2(^1\Delta_g)$ and $^1O_2(^1\sum_g^+)$

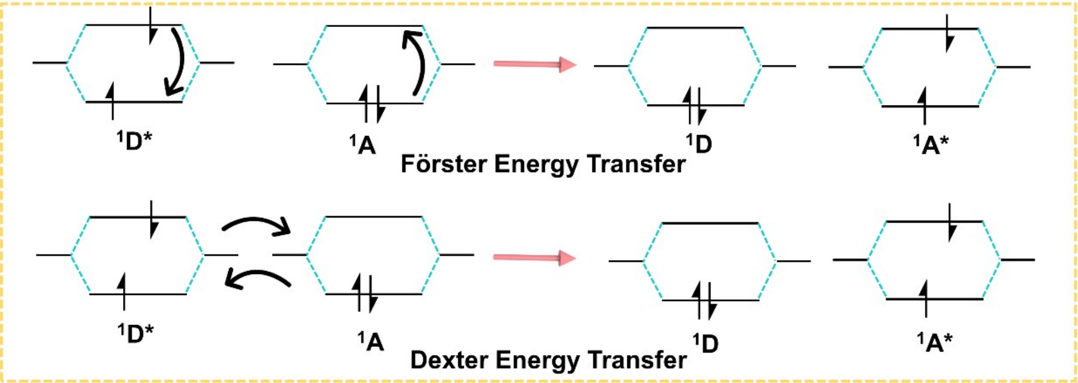

Figure S2. two ways of energy transfer

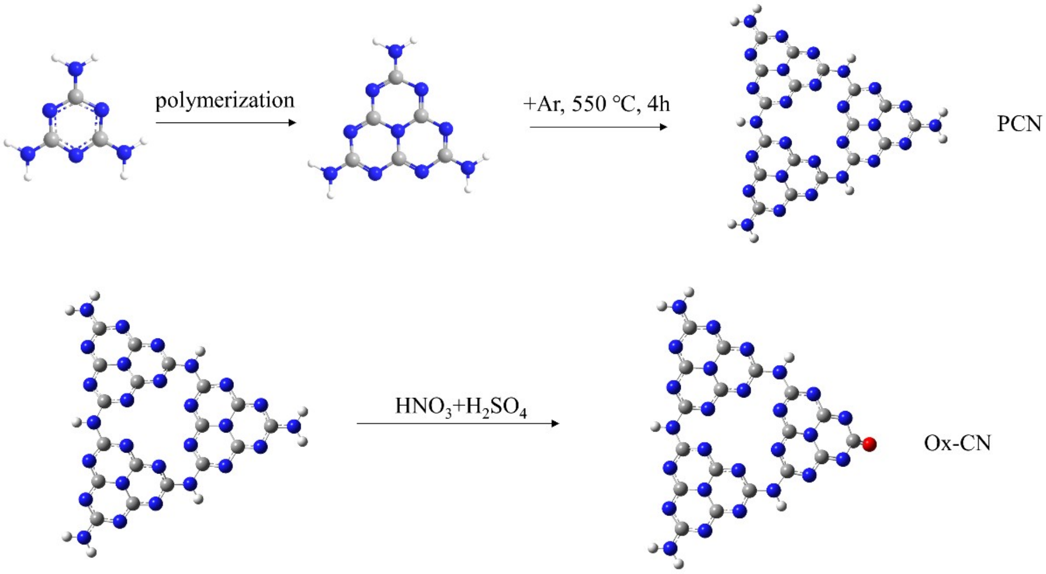

Figure S3. Schematic diagram of the synthesis of carbonylated carbon nitride (Ox-CN)

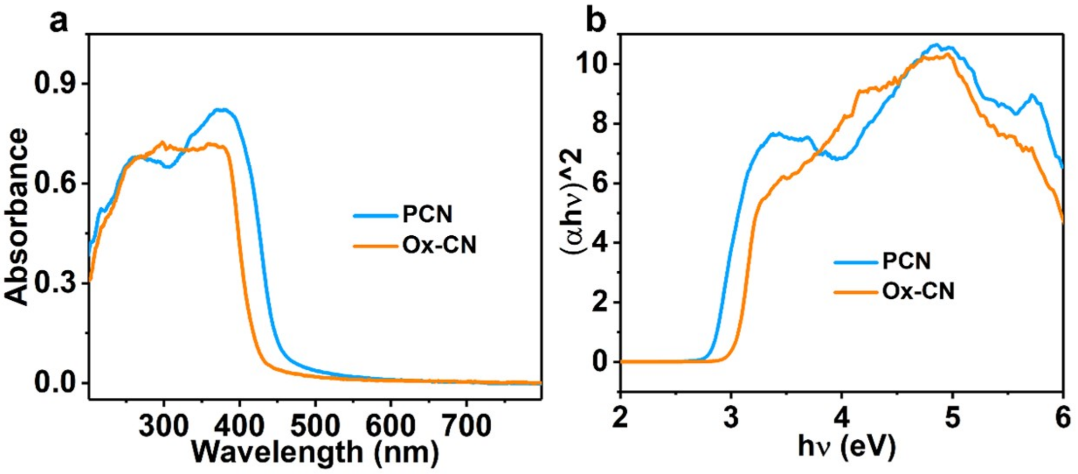

Figure S4. (a) UV-vis DRS and (b) plots of transformed Kubelka-Munk function versus photo energy of PCN and Ox-CN

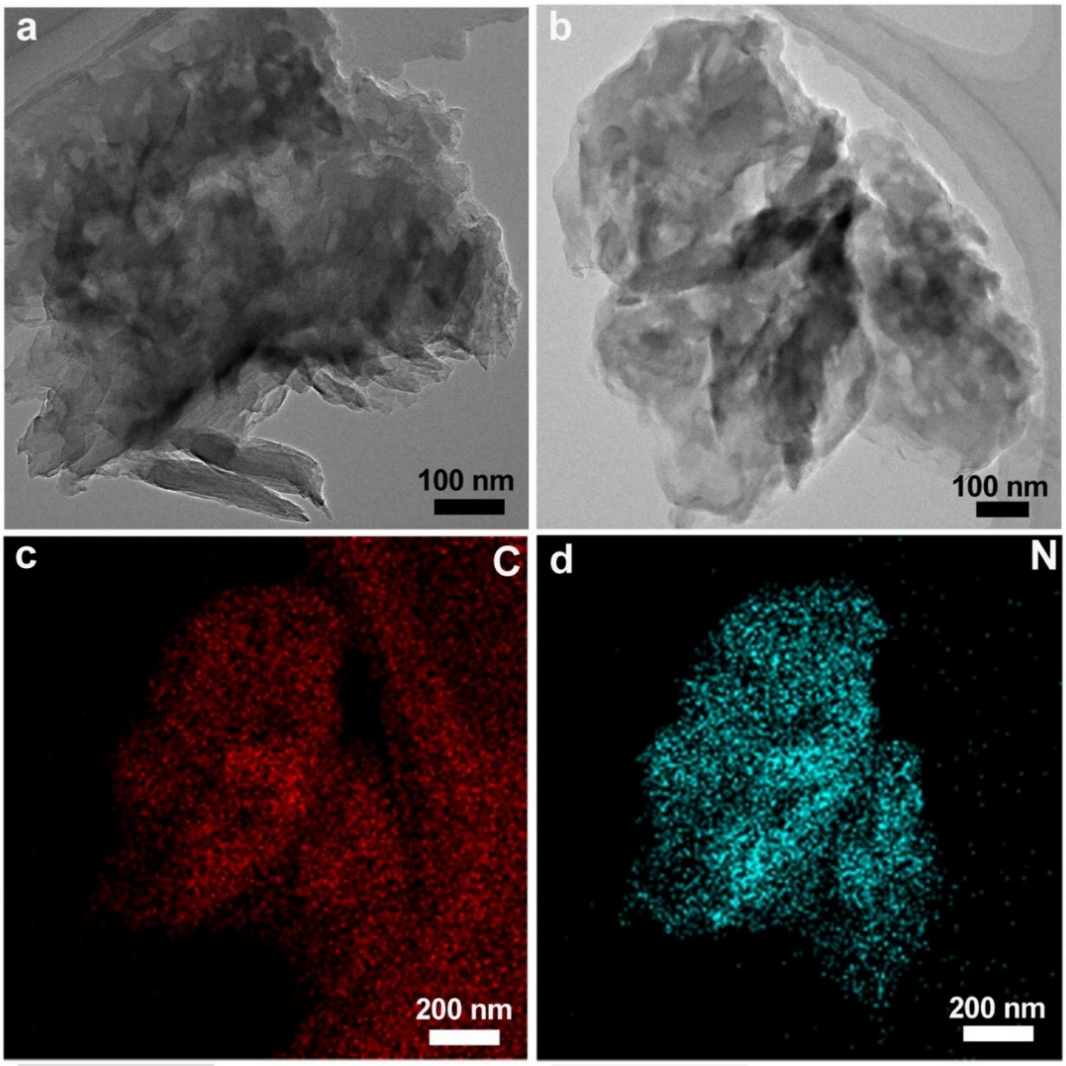

Figure S5. (a) and (b) the TEM images for PCN. (c) and (d) the elemental mapping images of PCN

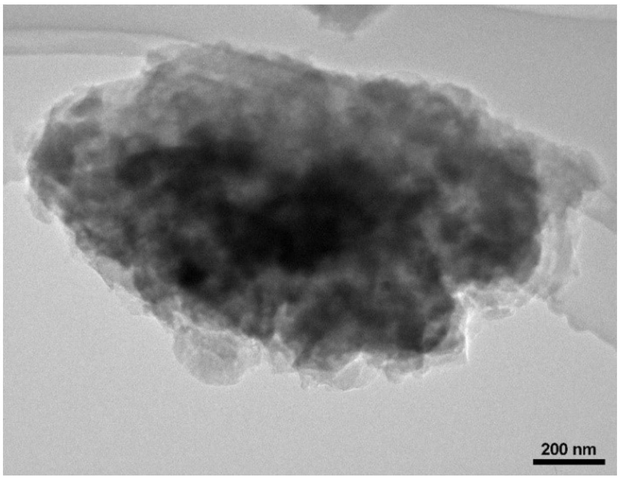

Figure S6. The TEM images for Ox-CN

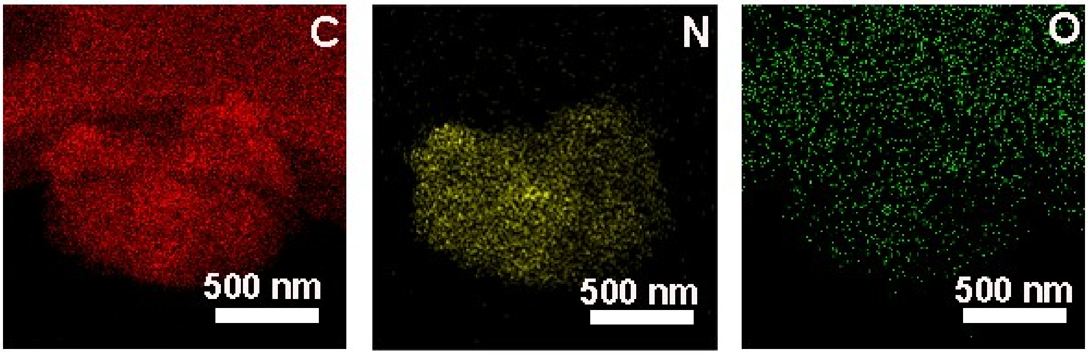

Figure S7. The elemental mapping images of Ox-CN

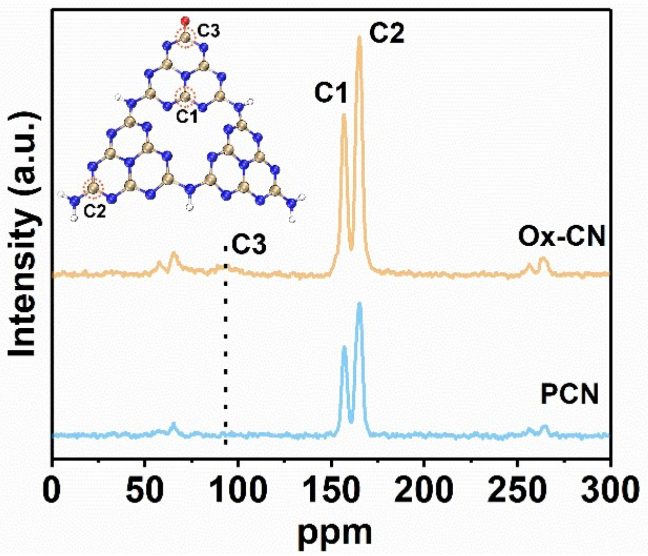

Figure S8. Solid-state ^{13}C NMR spectra of PCN and Ox-CN

The solid-state ^{13}C NMR spectra of PCN and Ox-CN (Figure R1) shows two peaks, the first peak at 157.1 ppm is ascribed to the (C1) atoms of melem(CN_3), whereas the second one at 165.4 ppm is attributed to the (C2) atoms of [$CN_2(NH_x)$] [6]. Moreover, compared with pure PCN, new C3 peak assignable to the incorporated carbonyl carbon in the Ox-CN network are clear visible at approximately 93.6 ppm.

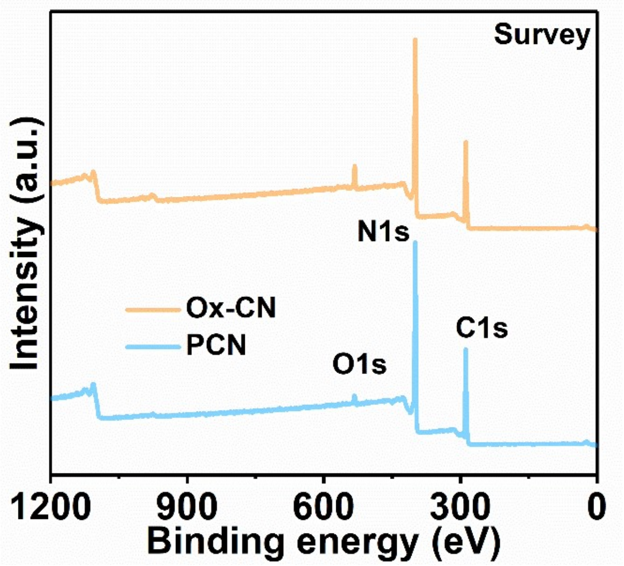

Figure S9. XPS survey spectra for PCN and Ox-CN

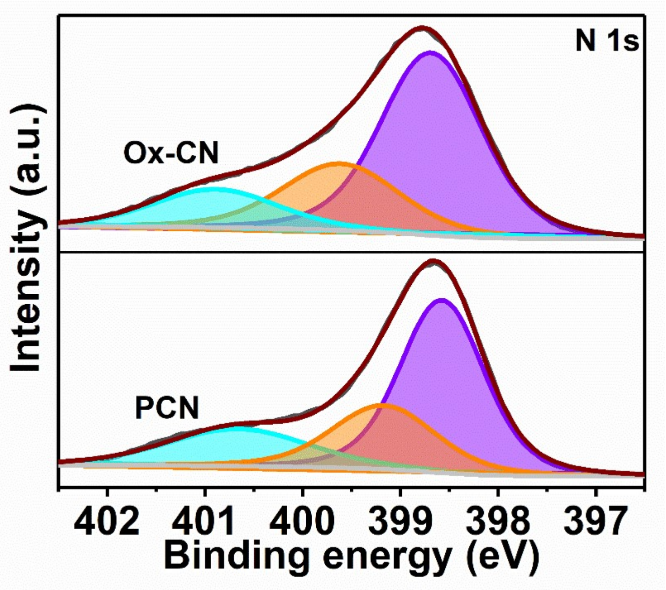

Figure S10. High resolution XPS spectra of N1s for PCN and Ox-CN

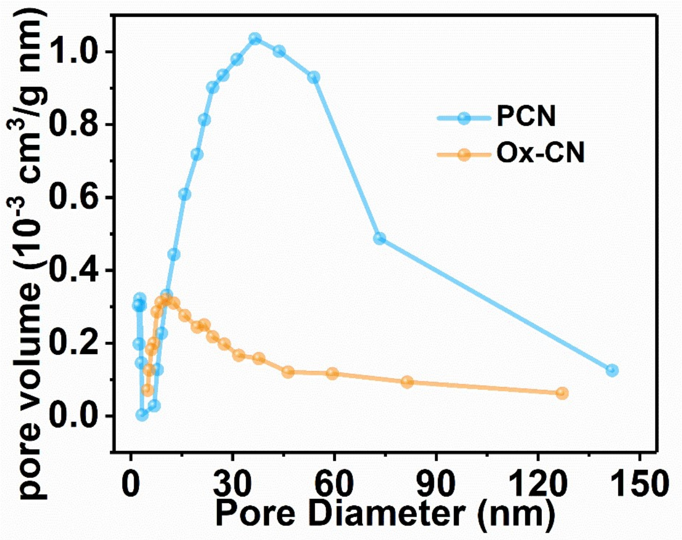

Figure S11. The pore size distribution of PCN and Ox-CN

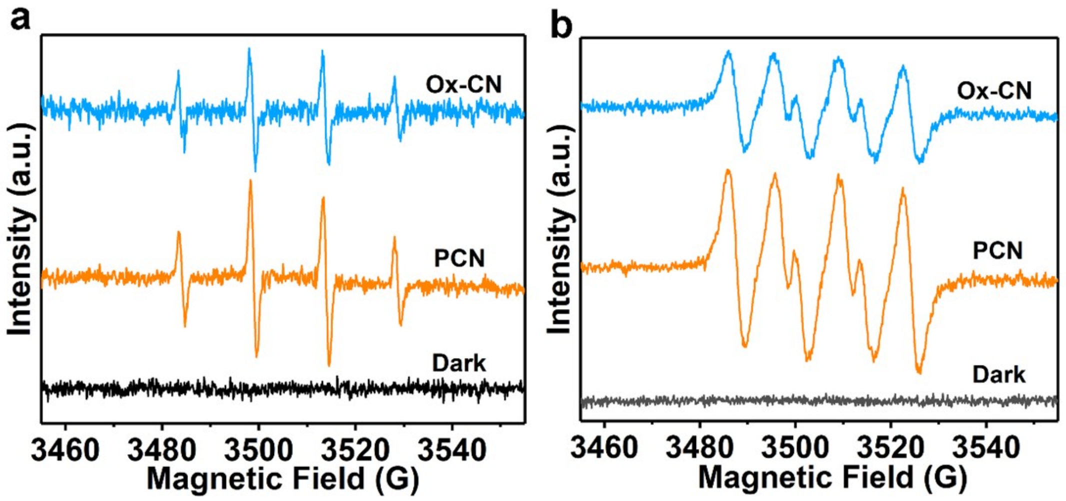

Figure S12. Spin-trapping spectra of (a) DMPO-$\cdot$OH and (b) DMPO-$\cdot O_2^-$ in different photo reaction systems

As the more direct evidence to identify the generated ROSs, electron spin resonance (ESR) measurements were performed on both Ox-CN and PCN. 2,2,6,6-tetramethylpiperidine (TEMP) was selected as the trapping agent to examine $^1O_2$ generation in the system. As shown in Figure S12, the ESR spectrum of Ox-CN displays an enhancement 1:1:1 triplet signal in comparison with PCN. Besides, 5,5-dimethyl-1-pyrroline-N-oxide (DMPO) was applied to detect the possible generation of $\cdot O_2^-$ and $\cdot$OH in the system. The ESR spectrum of PCN exhibits a 1:2:2:1 quartet characteristic in the presence of DMPO for the formation of DMPO-$\cdot$OH (Figure S12a). Meanwhile, six peaks for DMPO-$\cdot O_2^-$ detected in the ESR spectra were obviously higher in methanol dispersion of PCN than Ox-CN (Figure S12b). Thus, the observation of $^1O_2$ instead of $\cdot$OH and $\cdot O_2^-$ for Ox-CN strongly suggests that there should occur the suppression of charge-transfer process and meanwhile promote the generation of $^1O_2$.

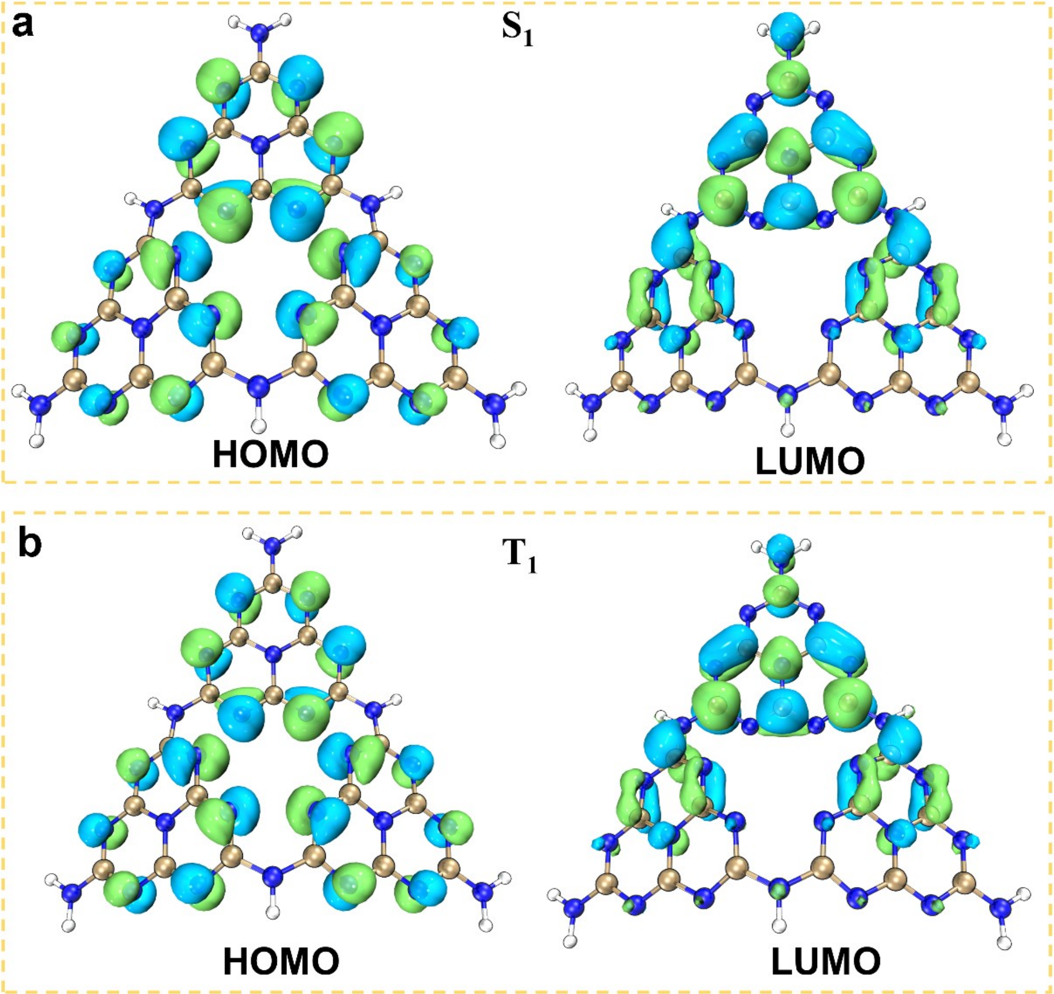

Figure S13. (a) The HOMO and LUMO for excited singlet states (S1) of PCN. (b) The HOMO and LUMO for excited triplet states (T1) of PCN. The iso-surface value is 0.03 e·Å^{-3}

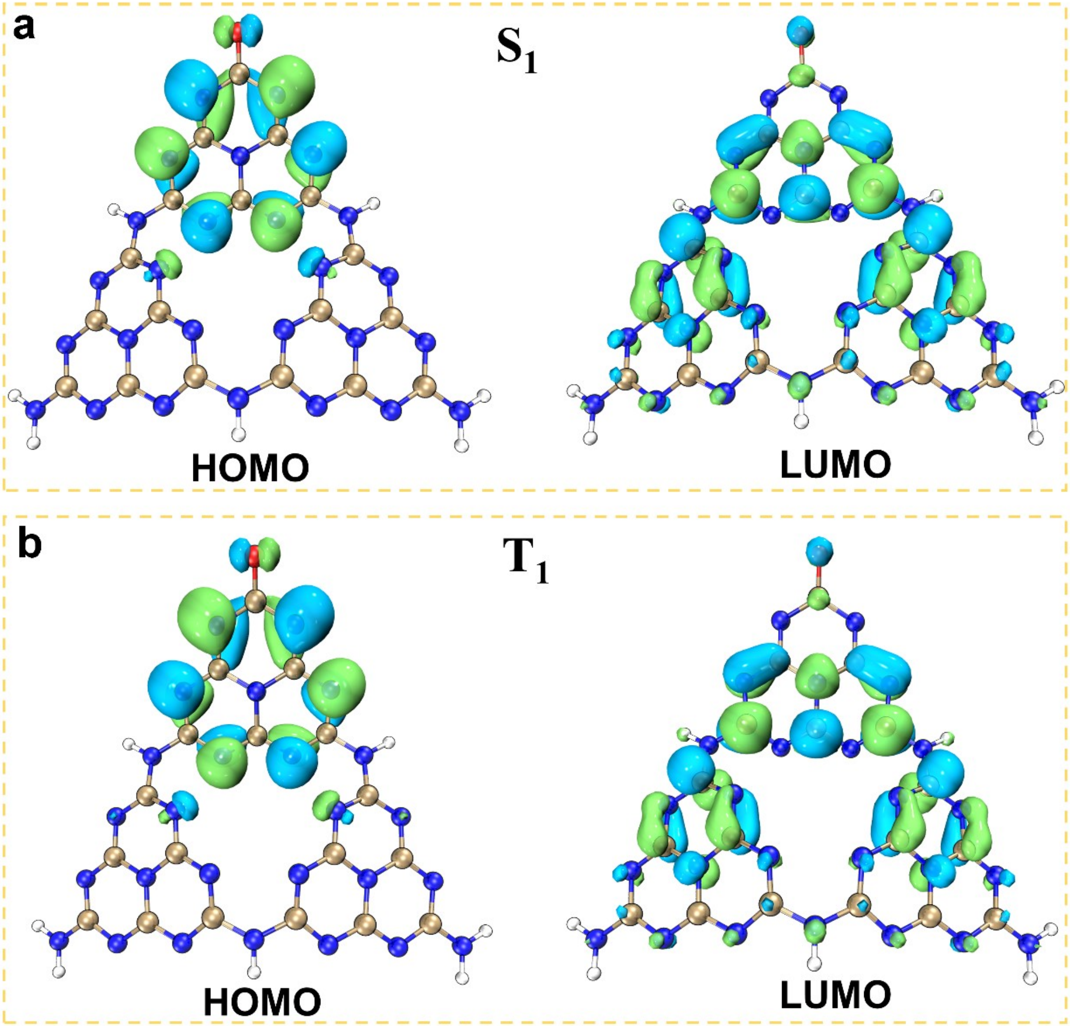

Figure S14. (a) The HOMO and LUMO for excited singlet states ($\mathbf{S_1}$) of Ox-CN. (b) The HOMO and LUMO for excited triplet states ($\mathbf{T_1}$) of Ox-CN. The iso-surface value is 0.03 e·Å^{-3}

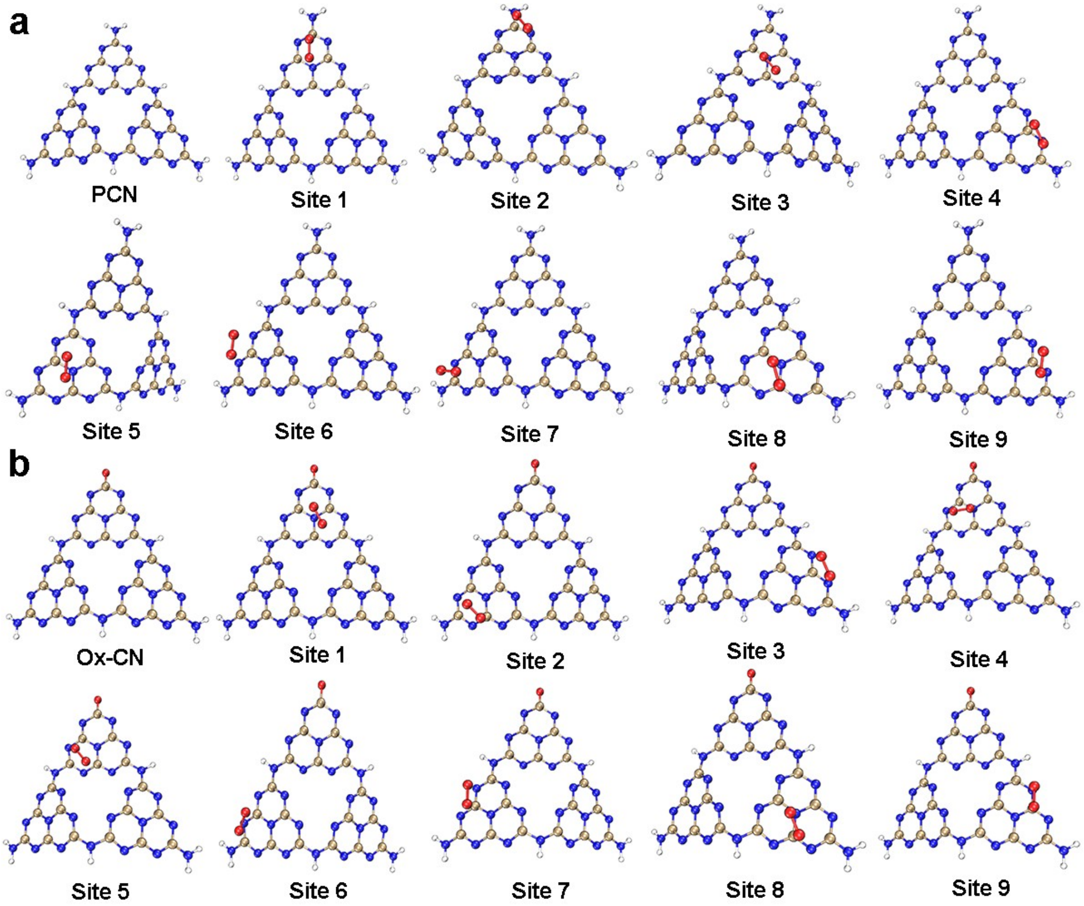

Figure S15. The possible adsorption sites of O_2 for PCN (a) and Ox-CN (b)

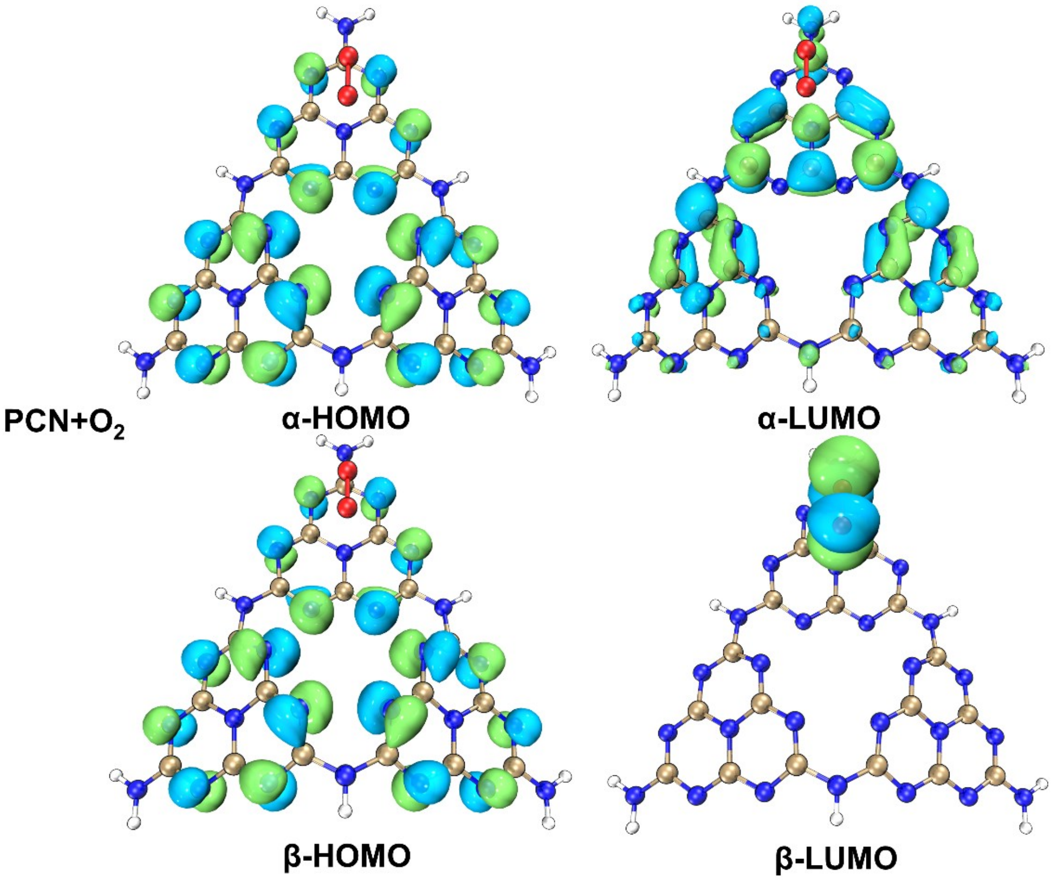

Figure S16. The α/β-HOMO and α/β-LUMO for the O_2 adsorbed PCN. The iso-surface value is 0.03 e·Å^{-3}

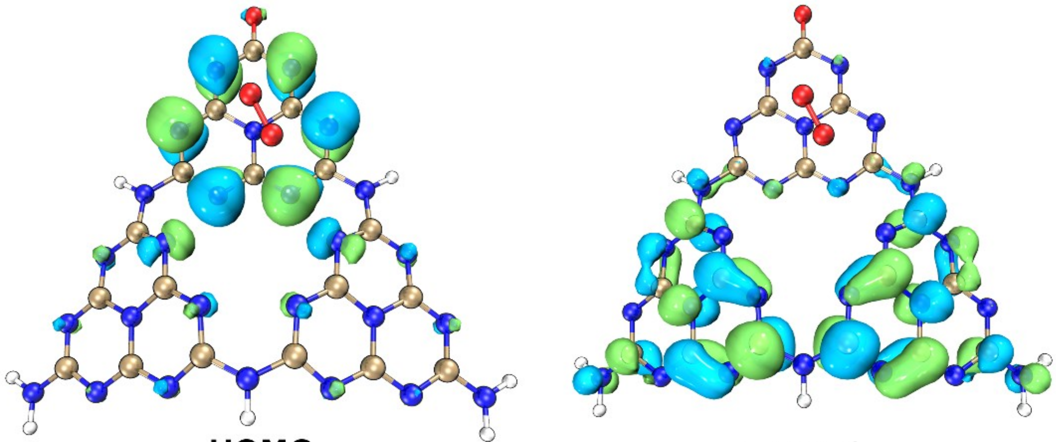

α-HOMO **α-LUMO**

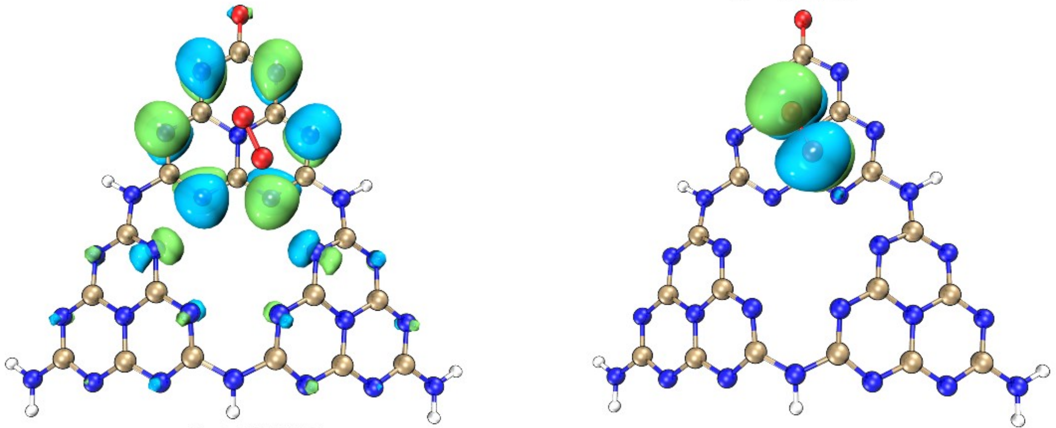

β-HOMO **β-LUMO**

Figure S17. The α/β-HOMO and α/β-LUMO for the O_2 adsorbed Ox-CN. The iso-surface value is 0.03 $e \cdot Å^{-3}$

Table S1 element analyses of PCN and Ox-CN sample

	PCN (atomic %)	Ox-CN (atomic %)
C	42.76	42.48
N	55.35	52.69
O	1.89	4.84

Table S2. Calculated SOCME between Triplets and Singlets for PCN

Root		<T|H_SO|S> (Re, Im) cm^{-1}			The total SOC integral (cm^{-1})
T	**S**	M$_s$=0	M$_s$=1	M$_s$=-1	
1	0	(0.00, -1.31)	(-0.04, 6.36)	(-0.04, -6.36)	9.08947193
1	1	(0.00, -0.00)	(0.33, 0.00)	(0.33, -0.00)	0.46669048
1	2	(0.00, -0.63)	(0.00, -0.55)	(0.00, 0.55)	1.00094955
1	3	(0.00, -0.00)	(-0.15, 0.00)	(-0.15, -0.00)	0.21213203
1	4	(0.00, 0.18)	(-0.00, 0.13)	(-0.00, -0.13)	0.25729361
1	5	(0.00, 0.00)	(0.12, 0.01)	(0.12, -0.01)	0.17029386
2	0	(0.00, 0.01)	(-6.23,-0.04)	(-6.23, 0.04)	8.81073777
2	1	(0.00, -0.72)	(0.00, -0.19)	(0.00, 0.19)	0.76850504
2	2	(0.00, -0.00)	(-0.32, -0.00)	(-0.32, 0.00)	0.45254834
2	3	(0.00,-0.53)	(0.00, 0.24)	(0.00, -0.24)	0.62936476
2	4	(0.00, -0.01)	(-0.63, -0.01)	(-0.63, 0.01)	0.89112289
2	5	(0.00, 0.94)	(-0.01, 1.15)	(-0.01, -1.15)	1.87851005
3	0	(0.00, -0.46)	(-0.01, -0.87)	(-0.01, 0.87)	1.31362095
3	1	(0.00, 0.00)	(0.28, -0.00)	(0.28, 0.00)	0.3959798
3	2	(0.00, -0.49)	(-0.00, 0.80)	(-0.00, -0.80)	1.23292336
3	3	(0.00, -0.00)	(0.16, -0.00)	(0.16, 0.00)	0.22627417
3	4	(0.00, -3.19)	(0.00, -2.44)	(0.00, 2.44)	4.69928718
3	5	(0.00, -0.05)	(0.33, -0.03)	(0.33, 0.03)	0.47127487
4	0	(0.00,-0.00)	(1.66, 0.02)	(1.66, -0.02)	2.34776489
4	1	(0.00, -0.07)	(-0.00, 0.59)	(-0.00, -0.59)	0.83731714
4	2	(0.00, -0.00)	(-0.04, 0.00)	(-0.04, -0.00)	0.05656854
4	3	(0.00, -2.12)	(0.00, -1.35)	(0.00, 1.35)	2.85296337
4	4	(0.00, -0.00)	(-0.56, -0.01)	(-0.56, 0.01)	0.79208585
4	5	(0.00, -0.10)	(-0.01, -0.02)	(-0.01, 0.02)	0.10488088
5	0	(0.00, -0.00)	(-2.50, 0.00)	(-2.50, -0.00)	3.53553391
5	1	(0.00, 1.21)	(-0.00, -0.03)	(-0.00, 0.03)	1.21074357
5	2	(0.00, 0.01)	(-0.06, 0.00)	(-0.06, -0.00)	0.06082763
5	3	(0.00, -0.18)	(-0.00, 0.42)	(-0.00, -0.42)	0.62064483
5	4	(0.00, 0.02)	(0.04, 0.01)	(0.04, -0.01)	0.06164414
5	5	(0.00, -1.51)	(0.00, -1.21)	(0.00, 1.21)	2.28217002

Table S3. Calculated SOCME between Triplets and Singlets for Ox-CN

<table>
<tr><th colspan="2">Root</th><th colspan="3"><T|H_SO|S> (Re, Im) cm^{-1}</th><th rowspan="2">The total SOC integral (cm^{-1})</th></tr>
<tr><th>**T**</th><th>**S**</th><th>M_s=0</th><th>M_s=1</th><th>M_s=-1</th></tr>
<tr><td>1</td><td>0</td><td>(0.00, -0.00)</td><td>(-2.26, -0.01)</td><td>(-2.26, 0.01)</td><td>3.19615</td></tr>
<tr><td>1</td><td>1</td><td>(0.00, 0.00)</td><td>(0.11, 0.00)</td><td>(0.11, 0.00)</td><td>0.16971</td></tr>
<tr><td>1</td><td>2</td><td>(0.00, 0.05)</td><td>(0.01, -1.03)</td><td>(0.01, 1.03)</td><td>1.45753</td></tr>
<tr><td>1</td><td>3</td><td>(0.00, 0.00)</td><td>(1.34, -0.01)</td><td>(1.34, 0.01)</td><td>1.8951</td></tr>
<tr><td>1</td><td>4</td><td>(0.00, 0.38)</td><td>(0.01, -3.90)</td><td>(0.01, 3.90)</td><td>3.91849</td></tr>
<tr><td>1</td><td>5</td><td>(0.00, -0.01)</td><td>(-2.81, -0.01)</td><td>(-2.81, 0.01)</td><td>3.97397</td></tr>
<tr><td>2</td><td>0</td><td>(0.00, -0.62)</td><td>(0.01, -1.90)</td><td>(0.01, 1.90)</td><td>1.99865</td></tr>
<tr><td>2</td><td>1</td><td>(0.00, -0.01)</td><td>(-0.00, 0.72)</td><td>(-0.00, -0.72)</td><td>1.01828</td></tr>
<tr><td>2</td><td>2</td><td>(0.00, -0.00)</td><td>(0.15, 0.00)</td><td>(0.15, -0.00)</td><td>0.21213</td></tr>
<tr><td>2</td><td>3</td><td>(0.00, 0.25)</td><td>(-0.01, 4.51)</td><td>(-0.01, -4.51)</td><td>4.51695</td></tr>
<tr><td>2</td><td>4</td><td>(0.00, -0.00)</td><td>(-0.02, -0.00)</td><td>(-0.02, 0.00)</td><td>0.02828</td></tr>
<tr><td>2</td><td>5</td><td>(0.00, 0.73)</td><td>(0.01, -3.83)</td><td>(0.01, 3.83)</td><td>3.89897</td></tr>
<tr><td>3</td><td>0</td><td>(0.00, -0.32)</td><td>(-0.02, -0.05)</td><td>(-0.02, 0.05)</td><td>0.32512</td></tr>
<tr><td>3</td><td>1</td><td>(0.00, 0.42)</td><td>(0.02, -4.53)</td><td>(0.02, 4.53)</td><td>4.54952</td></tr>
<tr><td>3</td><td>2</td><td>(0.00, -0.00)</td><td>(0.08, -0.03)</td><td>(0.08, 0.03)</td><td>0.12083</td></tr>
<tr><td>3</td><td>3</td><td>(0.00, -0.39)</td><td>(0.07, -20.83)</td><td>(0.07, 20.83)</td><td>20.8339</td></tr>
<tr><td>3</td><td>4</td><td>(0.00, -0.00)</td><td>(-0.04, -0.00)</td><td>(-0.04, 0.00)</td><td>0.05657</td></tr>
<tr><td>3</td><td>5</td><td>(0.00, -2.12)</td><td>(-0.04, 15.59)</td><td>(-0.04, -15.59)</td><td>15.7336</td></tr>
<tr><td>4</td><td>0</td><td>(0.00, 0.00)</td><td>(-0.61, -0.00)</td><td>(-0.61, 0.00)</td><td>0.86267</td></tr>
<tr><td>4</td><td>1</td><td>(0.00, -0.00)</td><td>(-1.26, 0.02)</td><td>(-1.26, -0.02)</td><td>1.78213</td></tr>
<tr><td>4</td><td>2</td><td>(0.00, -0.45)</td><td>(0.03, -8.81)</td><td>(0.03, 8.81)</td><td>8.82159</td></tr>
<tr><td>4</td><td>3</td><td>(0.00, 0.00)</td><td>(0.06, 0.03)</td><td>(0.06, -0.03)</td><td>0.09487</td></tr>
<tr><td>4</td><td>4</td><td>(0.00, -0.33)</td><td>(0.06, -18.57)</td><td>(0.06, 18.57)</td><td>18.5731</td></tr>
<tr><td>4</td><td>5</td><td>(0.00, 0.01)</td><td>(0.31, -0.09)</td><td>(0.31, 0.09)</td><td>0.44766</td></tr>
<tr><td>5</td><td>0</td><td>(0.00, -0.00)</td><td>(-1.52, -0.03)</td><td>(-1.52, 0.03)</td><td>2.15002</td></tr>
<tr><td>5</td><td>1</td><td>(0.00, 0.00)</td><td>(0.76, 0.01)</td><td>(0.76, -0.01)</td><td>1.0749</td></tr>
<tr><td>5</td><td>2</td><td>(0.00, -0.12)</td><td>(0.00, -0.07)</td><td>(0.00, 0.07)</td><td>0.15556</td></tr>
<tr><td>5</td><td>3</td><td>(0.00, -0.00)</td><td>(0.14, 0.06)</td><td>(0.14, -0.06)</td><td>0.21541</td></tr>
<tr><td>5</td><td>4</td><td>(0.00, -0.63)</td><td>(-0.03, 8.31)</td><td>(-0.03, -8.31)</td><td>8.33395</td></tr>
<tr><td>5</td><td>5</td><td>(0.00, 0.00)</td><td>(-0.11, -0.02)</td><td>(-0.11, 0.02)</td><td>0.15811</td></tr>
</table>

To investigate the effect of carbonyl functional groups, the spin-orbit coupling matrix element was proposed [7,8]. Among then, Ms=0, Ms=1 and Ms=-1 belong to three different spin magnetic quantum numbers of triplet states (Table S2 and Table S3). In addition, we also calculated five excited **S** and five excited **T** for PCN and Ox-CN, respectively.

For example, the <T_1|H_SO|S_2> for PCN is regarded as (0.00, -0.63), (0.00, -0.55) and (0.00, 0.55). The first item in parentheses is the real part (Re), and the following is imaginary part (Im). Therefore, assuming the total SOC integral is A.

According to the formula:

$$A = \sqrt{(0.00^2 + (-0.63)^2 + 0.00^2 + (-0.55)^2 + 0.00^2 + (-0.55)^2)} = 1.00094955$$

The <T|H_SO|S> reflect the magnitude of the SOC between the two electronic states T and **S**. The larger the <T|H_SO|S>, the stronger the interaction between two states, making it easier to transition. As shown in Figure 5c, most of the total SOC integral of Ox-CN are higher than those of PCN. This result demonstrates that the probability of interaction between **S** and **T** within Ox-CN has increased in comparison with PCN. The increase in interaction probability helps to enhance ISC, thus promoting the production of **T** excitons.

References

1. M. J. Frisch, G. W. Trucks, H. B. Schlegel, G. E. Scuseria, M. A. Robb, J. R. Cheeseman, G. Scalmani, V. Barone, G. A. Petersson, H. Nakatsuji, X. Li, M. Caricato, A. V. Marenich, J. Bloino, B. G. Janesko, R. Gomperts, B. Mennucci, H. P. Hratchian, J. V. Ortiz, A. F. Izmaylov, J. L. Sonnenberg, Williams, F. Ding, F. Lipparini, F. Egidi, J. Goings, B. Peng, A. Petrone, T. Henderson, D. Ranasinghe, V. G. Zakrzewski, J. Gao, N. Rega, G. Zheng, W. Liang, M. Hada, M. Ehara, K. Toyota, R. Fukuda, J. Hasegawa, M. Ishida, T. Nakajima, Y. Honda, O. Kitao, H. Nakai, T. Vreven, K. Throssell, J. A. Montgomery Jr., J. E. Peralta, F. Ogliaro, M. J. Bearpark, J. J. Heyd, E. N. Brothers, K. N. Kudin, V. N. Staroverov, T. A. Keith, R. Kobayashi, J. Normand, K. Raghavachari, A. P. Rendell, J. C. Burant, S. S. Iyengar, J. Tomasi, M. Cossi, J. M. Millam, M. Klene, C. Adamo, R. Cammi, J. W. Ochterski, R. L. Martin, K. Morokuma, O. Farkas, J. B. Foresman and D. J. Fox, *Journal*, 2016.
2. F. Weigend and R. Ahlrichs, *Phys. Chem. Chem. Phys.*, 2005, **7**, 3297-3305.
3. T. Lu and F. W. Chen, *J. Comput. Chem.*, 2012, **33**, 580-592.
4. W. Humphrey, A. Dalke and K. Schulten, *J Mol Graph Model*, 1996, **14**, 33-38.
5. P. C. Bunting, M. Atanasov, E. Damgaard-Moller, M. Perfetti, I. Crassee, M. Orlita, J. Overgaard, J. van Slageren, F. Neese and J. R. Long, *Science*, 2018, **362**, 1378-+.
6. C. Yang, B. Wang, L. Z. Zhang, L. Yin and X. C. Wang, *Angew. Chem., Int. Ed.,* 2017, 56, 6627-6631.
7. R. L. Feng, X. J. Yu and J. Autschbach, *J. Chem. Theory Comput.*, 2021, **17**, 7531-7544.
8. X. Gao, S. M. Bai, D. Fazzi, T. Niehaus, M. Barbatti and W. Thiel, *J. Chem Theory Comput.*, 2017, **13**, 515-524.